

## Chapter 6

# Macroscopic $pn$ Junctions

Shockley's 1949 paper heralded a new era in the history of semiconductor device physics and engineering[1]. Basic transport processes of a  $pn$  junction diode and transistor were presented in this paper. In the same issue, the first report appeared on the noise of a point contact transistor[2]. The observed noise figure was 50-70  $dB$  above the intrinsic noise limit! It took almost 60 years to suppress this excess noise (mainly due to  $1/f$  noise and surface recombination noise) and to obtain a noise figure very close to the theoretical limit. This intrinsic noise of a  $pn$  junction device is determined by the thermal noise in the bulk resistive region and the shot noise in the  $pn$  junction. In this chapter we will study the inherent noise of  $pn$  junction diodes, which sets a fundamental limit on the noise performance of various semiconductor  $pn$  junction devices, such as a semiconductor laser, photodiode, avalanche photodiode and bipolar transistor.

There are two distinct bias conditions for a  $pn$  junction diode: constant voltage operation and constant current operation. The former is realized when the junction differential resistance  $R_d$  is much larger than the source resistance  $R_s$ , and the latter is obtained in the opposite limit. There are two types of junction diodes: a macroscopic  $pn$  junction and mesoscopic  $pn$  junction. An electrostatic energy required for a single electron thermionic emission,  $q^2/2C$ , where  $C$  is a junction capacitance, is much smaller than the thermal energy  $k_B\theta$  in a macroscopic  $pn$  junction and the opposite is true for a mesoscopic  $pn$  junction. A junction diode features markedly different noise characteristics in such different bias conditions and junction sizes.

Consider a  $pn$  junction diode biased by a constant voltage source with a source resistance  $R_s$ , as shown in Fig. 6.1. If the source resistance  $R_s$  is much smaller than a diode differential resistance defined by

$$R_d \equiv \left( \frac{dI}{dV} \right)^{-1}, \quad (6.1)$$

where  $I$  and  $V$  are the junction current and the junction voltage, then the junction voltage  $V$  is always pinned by the source. There is no fluctuation in the junction voltage  $V$  due to the fast relaxation time ( $CR_s$ ) of an external circuit, but there is a fluctuation in the junction current  $I$ . This bias condition is referred to as "constant voltage operation." Standard theoretical studies on the noise characteristics of a  $pn$  junction diode have considered this mode of operation[3]; therefore, our analysis also starts with this bias condition.

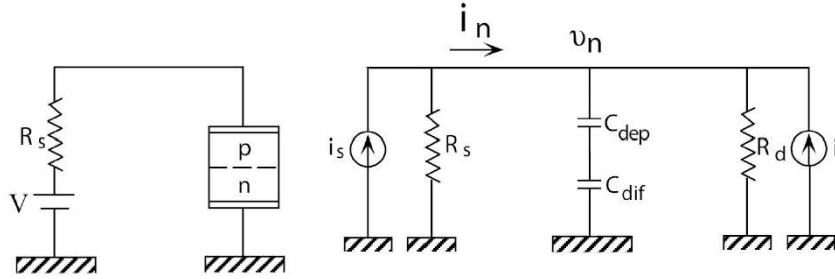


Figure 6.1: A  $pn$  junction diode biased by an external voltage source with a source resistance  $R_s$ , and a noise equivalent circuit.

On the other hand, when the source resistance  $R_s$  is much larger than the differential resistance  $R_d$  of the diode, there is no fluctuation in the junction current  $I$ . However, there is a fluctuation in the junction voltage  $V$  due to the slow relaxation time ( $CR_s$ ) of an external circuit. This bias condition is referred to as “constant current operation.”

There are two types of  $pn$  junctions which feature drastically different noise characteristics: macroscopic junctions and mesoscopic junctions. When a single-electron charging energy,  $q^2/2C$ , where  $C$  is the junction capacitance, is much smaller than the thermal characteristic energy  $k_B\theta$ , the behavior of each individual electron does not affect the junction dynamics. This is a macroscopic junction limit. On the other hand, when  $q^2/2C$  is much greater than  $k_B\theta$ , a so-called single-electron Coulomb blockade effect emerges and a single-electron thermionic emission event determines the junction dynamics. This is a mesoscopic junction limit.

Before we start the discussion on the noise of a  $pn$  junction diode, we will briefly revisit the noise of a vacuum diode, which connects a microscopic, random process inside a device and external circuit current noise.

## 6.1 Shot Noise in a Vacuum Diode: Revisit

### 6.1.1 Ramo Theorem

Suppose an electron is emitted from the cathode and is in transit to the anode in a vacuum diode (Fig. 6.2). Assume the source resistance,  $R_s$ , is zero, so the voltage across the diode is held constant,  $V_d(t) = V$ . As the electron moves from time  $t' = 0$  to  $t$ , the energy it gains from a constant electric field  $E = V/d$  is given by:

$$U' = \int_0^t dt' \vec{F} \cdot \vec{v} = q \int_0^t dt' E v(t) \quad , \quad (6.2)$$

where  $F = qE$  is an electro-static force on the electron,  $v(t)$  is the electron drift velocity, and  $d$  is the cathode-anode spacing. If the current in the external circuit is  $i(t)$ , the total energy supplied by the external voltage source is

$$U'' = \int_0^t dt' V i(t') \quad . \quad (6.3)$$

Since the kinetic energy gained by the electron should be equal to the energy provided by the voltage source, equating  $U' = U''$  yields:

$$\int_0^t dt' q E v(t) = \int_0^t dt' E d i(t') \quad . \quad (6.4)$$

From this equation, we have a relation between the circuit current  $i(t)$  and the electron velocity  $v(t)$ ,

$$i(t) = \frac{qv(t)}{d} \quad . \quad (6.5)$$

This relation is called Ramo theorem.

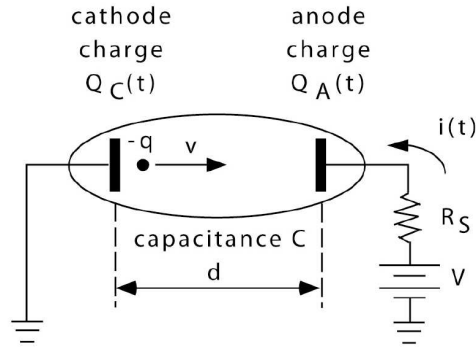


Figure 6.2: A vacuum diode biased by an external voltage source with a source resistance  $R_s$ .

We consider next the case that the external circuit has a finite source resistance,  $R_s$ , and the circuit relaxation time,  $\tau_c = R_s C$ , is much longer than the electron transit time,  $\tau_t$ , where  $C$  is the capacitance between the cathode and the anode of the vacuum diode.

For  $\tau_t \ll \tau_c$ , the voltage drop due to the electron transit event occurs “instantly,” whereas the relaxation through the external circuit is very slow. Immediately following the transit, the voltage across the vacuum diode is  $V - q/C$ , *i.e.*, the voltage at the anode is  $V_A(t) = V - q/C$  at  $t = 0$ . Using Kirchoff’s law, and noting that the current from the battery to the anode is equal to the current from the cathode to ground, we have

$$\frac{d}{dt} V_A(t) = -\frac{V_A(t)}{R_s C} + \frac{V}{R_s C} \quad , \quad (6.6)$$

and obtain the solution with the initial condition at  $t = 0$  as

$$V_A(t) = V - \frac{q}{C} e^{-t/R_s C} \quad . \quad (6.7)$$

The relaxation current in the external circuit is then

$$i(t) = \frac{V - V_A}{R_s} = \frac{q}{R_s C} e^{-t/R_s C} \quad . \quad (6.8)$$

We now calculate the surface charges of the cathode and the anode as a function of time for a single-electron traversal process in the following three cases:

- i) The electron drift velocity is assumed to be constant over the electron's transit from the cathode to the anode, and  $\tau_c \ll \tau_t$ .
- ii) The electron drift velocity is initially zero at the cathode and is accelerated by the constant applied electric field, and  $\tau_c \ll \tau_t$ .
- iii)  $\tau_c \gg \tau_t$ . In this case, we assume the electron transit to be an impulsive event.

Since there is a voltage of  $V$  across the vacuum diode, there is a surface charge of  $CV$  on the anode and  $-CV$  on the cathode, if no electron emission occurs. When an electron with charge  $-q$  is emitted from the cathode, it induces a net charge of  $+q$  on the cathode. If  $R_s = 0$ , this charge is compensated instantaneously by the current supplied from the external circuit. The surface charge on the cathode is:

$$Q_C(t) = -CV + q - \int_0^t dt' i(t') \quad . \quad (6.9)$$

For the case i): constant electron velocity, we perform the integration and obtain,

$$Q_C(t) = \begin{cases} -CV + q(1 - \frac{v}{d}t) & 0 < t < \frac{d}{v} \\ -CV & \text{otherwise} \end{cases} \quad . \quad (6.10)$$

The surface charge on the anode starts increasing by  $+q$  over the time  $\tau_t = d/v$ , due to the external current, from its  $t = 0$  value of  $CV$ . Then, it is compensated by the electron from the cathode. The surface charge on the anode is,

$$Q_A(t) = CV + \int_0^t dt' i(t') = \begin{cases} CV + q\frac{v}{d}t & 0 < t < \frac{d}{v} \\ CV & \text{otherwise} \end{cases} \quad . \quad (6.11)$$

Since the external voltage source supplies external current (without delay) to keep up with the change inside the diode, the voltage across the diode is kept constant.

For the case ii) we allow the electron to be accelerated by the electric field. The electron acquires a velocity,

$$v(t) = \frac{qE}{m}t \quad . \quad (6.12)$$

The transit time across the vacuum diode is obtained by the condition,

$$\int_0^d dr = \int_0^{\tau_t} dt' v(t') \quad . \quad (6.13)$$

Solving the above equation, we obtain

$$\tau_t = \sqrt{\frac{2md^2}{qV}} \quad . \quad (6.14)$$

The current can then be calculated as

$$i(t) = \frac{q}{d}v(t) = \frac{q^2V}{md^2}t \quad . \quad (6.15)$$

The surface charge on the cathode is,

$$\begin{aligned} Q_C(t) &= -CV + q - \int_0^t dt' i(t') \\ &= \begin{cases} -CV + q(1 - \frac{v(t)}{2d}t) & 0 < t < \tau_t \\ -CV & \text{otherwise} \end{cases} . \end{aligned} \quad (6.16)$$

The surface charge on the anode is:

$$\begin{aligned} Q_A(t) &= CV + \int_0^t dt' i(t') \\ &= \begin{cases} CV + \frac{qv(t)}{2d}t & 0 < t < \tau_t \\ CV & \text{otherwise} \end{cases} . \end{aligned} \quad (6.17)$$

Finally, for the case iii): impulsive electron transit, the charge on the anode is given by

$$Q_A(t) = CV_A(t) = \begin{cases} CV - qe^{-t/RC} & t > 0 \\ CV & t < 0 \end{cases} . \quad (6.18)$$

And on the cathode,

$$Q_C(t) = -CV_A(t) = \begin{cases} -CV + qe^{-t/RC} & t > 0 \\ -CV & t < 0 \end{cases} . \quad (6.19)$$

Here, the voltage across the diode has an RC relaxation.

### 6.1.2 Current Noise

If each electron emission event and its transport process are mutually independent, we can calculate the external current noise spectra for the above three cases by the Carson's theorem (Chapter 1).

i)  $\tau_c \ll \tau_t$  and constant  $v$

The Carson theorem states that for a random pulse train  $i(t) = \sum_{k=1}^K a_k f(t - t_k)$  with identical pulse shape  $f(t)$ , the unilateral power spectrum is given by,

$$S(\omega) = 2\nu\bar{a}^2 |F(i\omega)|^2 + 4\pi \left[ \nu\bar{a} \int_{-\infty}^{\infty} dt f(t) \right]^2 \delta(\omega) , \quad (6.20)$$

where  $\nu$  is the average rate of electron emission and  $F(i\omega)$  is the Fourier transform of  $f(t)$ . In this case, each current pulse is given by

$$f(t) = \begin{cases} \frac{qv}{d} & 0 < t < \frac{d}{v} \\ 0 & \text{otherwise} \end{cases} ,$$

and the Fourier transform is

$$F(i\omega) = qe^{-i\omega d/2v} \frac{\sin(\omega d/2v)}{(\omega d/2v)} . \quad (6.21)$$

Using Eq. (6.20), we obtain

$$S_i(\omega) = 2\nu q^2 \frac{\sin^2(\omega d/2v)}{(\omega d/2v)^2} + 4\pi\nu^2 q^2 \delta(\omega) \quad . \quad (6.22)$$

Since the average electron emission rate is  $\nu$ , the current is given by  $I = q\nu$ . Therefore Eq. (6.22) can be written as

$$S_i(\omega) = 2qI \left[ \text{sinc}(\omega d/2v) \right]^2 + 4\pi I^2 \delta(\omega) \quad . \quad (6.23)$$

In the low-frequency limit,  $0 < \omega \ll v/d$ , since  $\lim_{x \rightarrow 0} \frac{\sin x}{x} = 1$ , we have

$$S_i(\omega \ll v/d) = 2qI \quad , \quad (6.24)$$

which is full shot noise.

ii)  $\tau_c \ll \tau_t$  and accelerated  $v$

In this case, each current pulse is given by

$$a = \frac{q^2 V}{d^2 m} \text{ and } f(t) = \begin{cases} t & 0 < t < T_{\text{tr}} \\ 0 & \text{otherwise} \end{cases} \quad .$$

It follows that:

$$\overline{a^2} = a^2 \quad , \quad (6.25)$$

$$F(i\omega) = i\tau_t \frac{e^{-i\omega\tau_t}}{\omega} - \frac{1 - e^{-i\omega\tau_t}}{\omega^2} \quad , \quad (6.26)$$

$$|F(i\omega)|^2 = \frac{2 + \omega^2 \tau_t^2 - 2\omega\tau_t \sin(\omega\tau_t) - 2\cos(\omega\tau_t)}{\omega^4} \quad . \quad (6.27)$$

Plugging into the unilateral power spectral density as per the Carson theorem, we have

$$S_i(\omega) = 2\nu \left( \frac{q^2 V}{d^2 m} \right)^2 \left[ \frac{2 + \omega^2 \tau_t^2 - 2\omega\tau_t \sin(\omega\tau_t) - 2\cos(\omega\tau_t)}{\omega^4} \right] + 4\pi\nu^2 q^2 \delta(\omega) \quad . \quad (6.28)$$

We use the following Taylor series expansions

$$\sin(\omega\tau_t) = \omega\tau_t - \frac{1}{3!}(\omega\tau_t)^3 + O(\omega^5) \quad ,$$

$$\cos(\omega\tau_t) = 1 + \frac{1}{2!}(\omega\tau_t)^2 + \frac{1}{4!}(\omega\tau_t)^4 + O(\omega^6) \quad ,$$

in the small frequency limit, to rewrite the power spectral density as

$$S_i(\omega) = 2\nu \left( \frac{q^2 V}{d^2 m} \right)^2 \left( \frac{2}{3!}\tau_t^4 - \frac{2}{4!}\tau_t^4 + O(\omega^5) \right) + 4\pi\nu^2 q^2 \delta(\omega) \quad . \quad (6.29)$$

In the low-frequency limit, we can ignore  $O(\omega^5)$ , and we have

$$S_i \left( \omega \ll \frac{1}{\tau_t} \right) = 2qI \quad . \quad (6.30)$$

which is again full shot noise.

iii)  $\tau_t \ll \tau_c$ , impulsive electron transit

In this case, each current pulse is given by

$$f(t) = \begin{cases} \frac{q}{CR_s} e^{-t/R_s C} & t > 0 \\ 0 & t < 0 \end{cases} ,$$

and the Fourier transform is

$$F(i\omega) = \frac{q}{1 + i\omega R_s C} . \quad (6.31)$$

The power spectral density is then,

$$S_i(\omega) = 2qI \frac{1}{1 + \omega^2 R_s^2 C^2} + 4\pi I^2 \delta(\omega) . \quad (6.32)$$

In the low-frequency limit, we obtain

$$S_i(\omega \ll 1/R_s C) = 2qI , \quad (6.33)$$

which is again full shot noise.

The origin of shot noise in a vacuum diode is the statistical independence of electron emission events at the cathode. If there is a statistical dependence between the electron emission events, this dependence manifests itself as a negative feedback process in which subsequent electron emissions are modulated by earlier events. There are two notable effects:

- a) a space-charge effect in the  $\tau_t \gg \tau_c$  limit, in which the existence of many electrons in the vacuum diode creates a potential modulation such that the rate of electron emissions is substantially smoothed.
- b) a memory effect in the external circuit in the  $\tau_c \gg \tau_t$  limit, in which the slow recovery of the voltage across the vacuum diode suppresses the rate of the subsequent electron emissions.

In both cases, the shot noise is suppressed to below full shot noise value. We will see the essentially same physics, full shot noise under constant voltage operation and sub-shot noise under constant current operation, in a  $pn$  junction diode in the remaining part of this chapter.

## 6.2 $pn$ Junction Diodes Under Constant Voltage Operation

### 6.2.1 Current-Voltage and Capacitance-Voltage Characteristics

The noise characteristics of a  $p^+-N$  heterojunction with a heavily  $p$ -doped narrow bandgap material and lightly  $n$ -doped wide bandgap material (Fig. 6.3) will be studied in this section, rather than a conventional  $p-n$  homojunction. This is because this specific junction structure is used in various important semiconductor devices such as a double-heterostructure semiconductor laser and heterojunction bipolar transistor. The extension of the following analysis to a  $pn$  homojunction is straightforward[3].

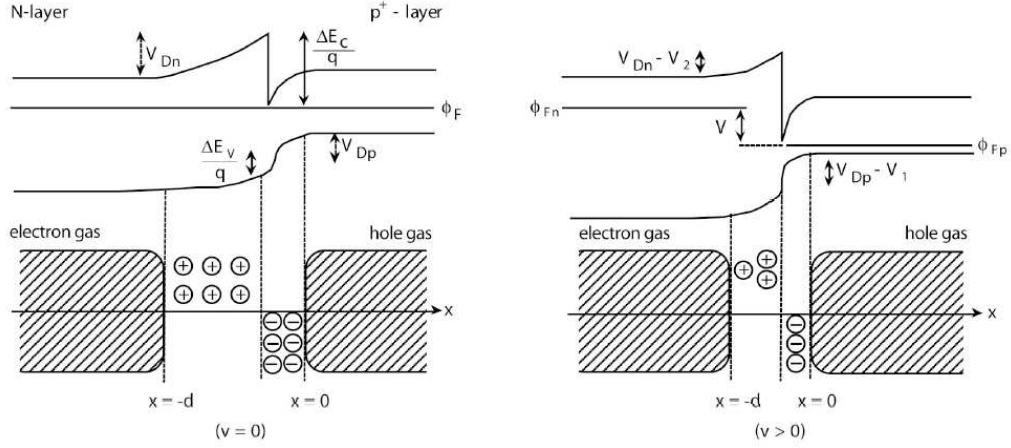


Figure 6.3: A  $p^+N$  heterostructure junction diode at equilibrium ( $V = 0$ ) and under a forward bias condition ( $V > 0$ ).

The band diagram of a  $p^+N$  heterojunction diode at a zero bias condition ( $V = 0$ ) and a forward bias condition ( $V > 0$ ) are shown in Fig. 6.3. The built-in potential  $V_D$  is divided into the potentials in the  $p^+$ - and  $N$ -layers[4]:

$$V_{Dp} = \frac{V_D}{K} \quad , \quad (6.34)$$

$$V_{Dn} = V_D \left(1 - \frac{1}{K}\right) \quad , \quad (6.35)$$

where

$$K = 1 + \frac{\varepsilon_1(N_{A1}^- - N_{D1}^+)}{\varepsilon_2(N_{D2}^+ - N_{A2}^-)} \quad . \quad (6.36)$$

Here,  $\varepsilon_1$ ,  $N_{A1}$ , and  $N_{D1}$  are the dielectric constant, acceptor concentration, and donor concentration of the  $p^+$ -layer, and  $\varepsilon_2$ ,  $N_{A2}$ , and  $N_{D2}$  are those of the  $N$ -layer. Since a  $p^+N$  diode satisfies  $\varepsilon_1 > \varepsilon_2$  and  $N_{A1}^- - N_{D1}^+ \gg N_{D2}^+ - N_{A2}^-$ , we have  $K \gg 1$ . Consequently, the built-in potential  $V_D$  is mainly supported in the  $N$ -layer, i.e.,  $V_{Dn} \simeq V_D$  and  $V_{Dp} \simeq 0$ . The transmitted electron flux from the  $N$ -layer to the  $p^+$ -layer across the potential barrier height  $V_{Dn}$  should be equal to the transmitted electron flux from the  $p^+$ -layer to the  $N$ -layer across the potential barrier  $\Delta E_c/q$  because there is no net current at  $V = 0$ .

When a forward bias ( $V > 0$ ) is applied, only the potential barrier seen by the electrons in the  $N$ -layer decreases to  $V_{Dn} - V_2 \simeq V_D - V$ , where the applied voltage supported in the  $N$ -layer is  $V_2 = V \left(1 - \frac{1}{K}\right) \simeq V$ . The electron density at the edge of the depletion layer ( $x = 0$ ) in the  $p^+$ -layer is given by[4]

$$n_p = X n_{N0} \exp\left(-\frac{V_D - V}{V_T}\right) = n_{p0} \exp\left(\frac{V}{V_T}\right) \quad , \quad (6.37)$$

where  $V_T = \frac{k_B \theta}{q}$  is the thermal voltage and

$$n_{p0} = X n_{N0} \exp\left(-\frac{V_D}{V_T}\right) \quad , \quad (6.38)$$

is the thermal equilibrium electron density in the  $p^+$ -layer.  $X$  is the transmission coefficient of an electron at the heterojunction interface and  $n_{N0}$  is the electron density at the edge of the depletion layer ( $t = -d$ ) in the  $N$ -layer which is equal to the thermal equilibrium electron density in the  $N$ -layer.

The excess electron density Eq. (6.37) at  $x = 0$  diffuses towards  $x = W$  (not shown in Fig. 6.3), where a  $p$ -side metal contact is located. The distribution of the excess electron density  $n(x, t)$  obeys[4]

$$\frac{\partial}{\partial t} n(x, t) = -\frac{n(x, t) - n_{p0}}{\tau_n} - \frac{1}{q} \frac{\partial}{\partial x} i_n(x, t) \quad , \quad (6.39)$$

where  $\tau_n$  is the electron lifetime and, since there is no electric field in the neutral  $p^+$ -layer, the current  $i_n(x, t)$  is carried only by a diffusion component

$$i_n(x, t) = -q D_n \frac{\partial}{\partial x} n(x, t) \quad . \quad (6.40)$$

Here,  $D_n$  is the electron diffusion constant. Solving Eqs. (6.39) and (6.40) with the boundary conditions,

$$n_p = \begin{cases} n_{p0} \exp\left(\frac{V}{V_T}\right) & \text{at } x = 0 \\ n_{p0} & \text{at } x \gg L_n \end{cases} \quad , \quad (6.41)$$

the steady-state solution for  $n(x)$  is now given by

$$n_p(x) = n_{p0} + (n_p - n_{p0}) e^{-x/L_n} \quad , \quad (6.42)$$

where  $L_n = \sqrt{D_n \tau_n}$  is the electron diffusion length. The junction current density is determined by the diffusion current Eq. (6.40) at  $x = 0$ :

$$i \equiv i_n(x = 0) = \frac{q D_n}{L_n} (n_p - n_{p0}) = \frac{q D_n n_{p0}}{L_n} \left( e^{\frac{V}{V_T}} - 1 \right) \quad . \quad (6.43)$$

The total current  $I = Ai$  vs. the junction voltage  $V$  is plotted in Fig. 6.4, where  $A$  is a cross-sectional area.

The differential resistance  $R_d$ , defined by  $\left(\frac{dI}{dV}\right)^{-1}$ , is approximately given by  $V_T/I$  under a reasonably strong forward bias condition. The diffusion capacitance  $C_{dif}$  of the diode is defined as the voltage derivative of the total excess minority carrier charge:

$$\begin{aligned} C_{dif} &\equiv \frac{d}{dV} Q_{(\text{minority carrier})} = A \frac{d}{dV} \left[ q \int_0^\infty [n_p(x) - n_{p0}] dx \right] \\ &= \frac{A q L_n n_{p0}}{V_T} e^{\frac{V}{V_T}} \\ &\simeq \frac{I}{V_T} \tau_n \quad . \end{aligned} \quad (6.44)$$

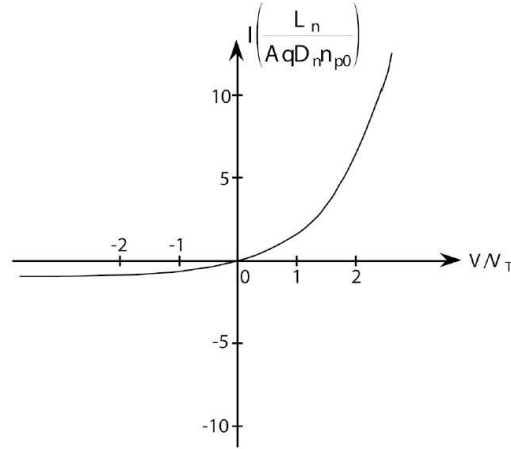


Figure 6.4: A current-voltage characteristic of a  $p^+-N$  junction diode.

The  $CR$  time constant characterized by the differential resistance  $R_d$  and the diffusion capacitance  $C_{dif}$  is thus equal to the electron lifetime  $\tau_n$ .

The depletion-layer capacitance  $C_{dep}$  of the diode is defined as the voltage derivative of the total space charge in the depletion region:

$$\begin{aligned}
 C_{dep} &\equiv \frac{d}{dV} Q_{(\text{space charge})} \\
 &= \frac{\varepsilon_2}{W_{dep}} A \\
 &= \sqrt{\frac{q\varepsilon_2 N_{D2}}{2(V_D - V)}} A
 \end{aligned} \tag{6.45}$$

Here,  $W_{dep} = \sqrt{\frac{2\varepsilon_2}{qN_{D2}}(V_D - V)}$  is the depletion layer width in the  $N$ -layer. The capacitance contributed by the depletion layer in the  $p^+$ -layer is neglected. The  $CR$  time constant characterized by the differential resistance  $R_d$  and the depletion layer capacitance  $C_{dep}$  is equal to the thermionic emission time  $\tau_{te}$ , the physical meaning of which will be discussed later in this chapter.

It will be shown that the thermionic emission time  $\tau_{te} = C_{dep}R_d$  is a key parameter for determining the noise characteristics of a  $pn$  junction diode under weak forward bias, while the minority-carrier lifetime  $\tau_n = C_{dif}R_d$  is a key parameter for determining the noise characteristics of a  $pn$  junction diode under strong forward bias. This conclusion is somewhat expected, because the junction capacitance of a  $pn$  junction is determined by the depletion-layer capacitance under weak forward bias and by the diffusion capacitance under strong forward bias.

### 6.2.2 Thermal Diffusion Noise

When a  $pn$  junction is biased by a constant voltage source, the electron densities at  $x = 0$  (edge of the depletion layer) and  $x = W$  ( $p$ -side metal contact) are always held constant to  $n_{p0} e^{V/V_T}$  and  $n_{p0}$ , respectively. The electron density fluctuates, however, between  $x = 0$  and  $x = W$  due to microscopic random electron motion induced by thermal agitation and by generation and recombination processes. In order to keep the boundary conditions at  $x = 0$  and  $x = W$  and to restore the steady-state electron distribution in this bulk  $p^+$ -region, the relaxation current pulse flows in the entire  $p^+$ -region between  $x = 0$  and  $x = W$ . This relaxation current inside the  $p^+$ -region results in the departure from charge neutrality of this region, unless we consider the carrier injection by the external circuit. Indeed, to sustain the charge neutrality of the bulk region, the external circuit current is induced. Our analysis in this and next sections follow the argument presented in ref. [3].

If an electron makes a transit over a small distance  $\ell_f$  between collisions with the lattice, an instantaneous current  $q\delta(t)$  flows at the two locations  $x = x'$  and  $x = x' + \ell_f$ , as shown in Fig. 6.5. This instantaneous current creates the departure from the steady-state electron distribution Eq. (6.42) and triggers the relaxation current to remove this deviation in the entire  $p^+$ -region between  $x = 0$  and  $x = W$ , which, after a reasonably short time, restores the steady-state electron distribution Eq. (6.42). The electron distribution deviation  $n'(x, t) = n(x, t) - n_{p0}(x)$ , which results in such a relaxation current in the entire region, satisfies the diffusion equation Eq. (6.39) and the boundary conditions  $n' = 0$  at  $x = 0$  and  $x = W$  at all time. The Fourier transform of the diffusion equation Eq. (6.39)

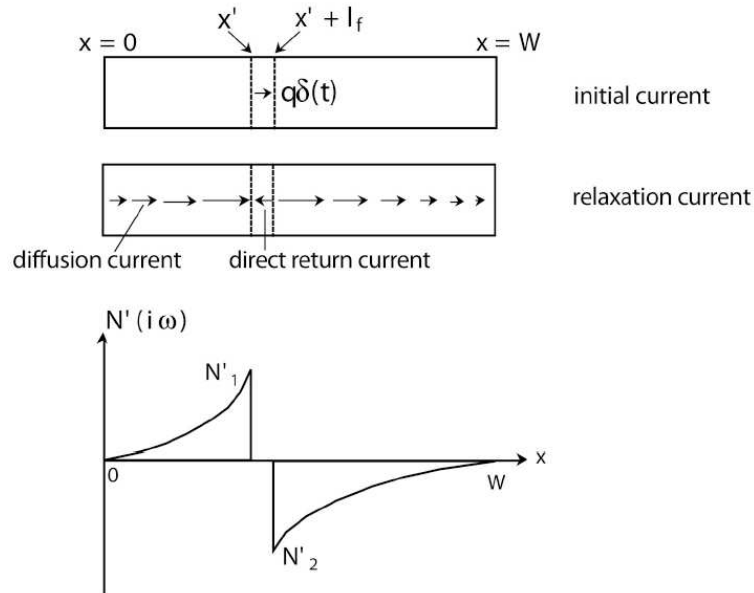


Figure 6.5: The initial current and subsequent relaxation current for a thermal diffusion process of a minority carrier.

is given by

$$\frac{\partial^2}{\partial x^2} N'(i\omega) = \frac{1}{L^2} N'(i\omega) \quad , \quad (6.46)$$

where  $N'(i\omega)$  is the Fourier transform of  $n'(x, t)$  and

$$L^2 = \frac{L_n^2}{1 + i\omega\tau_n} \quad . \quad (6.47)$$

The Fourier transform of the relaxation currents  $i'_1(t)$  at  $x = x'$  and  $i'_2(t)$  at  $x = x' + \ell_f$  are expressed in terms of the Fourier-transformed electron density deviations  $N'_1(i\omega)$  at  $x = x'$  and  $N'_2(i\omega)$  at  $x = x' + \ell_f$ [3]:

$$I'_1(i\omega) = qD_n \frac{\partial N'(i\omega)}{\partial x} \Big|_{x=x'} = k_1 N'_1(i\omega) \quad , \quad (6.48)$$

$$I'_2(i\omega) = qD_n \frac{\partial N'(i\omega)}{\partial x} \Big|_{x=x'+\ell_f} = -k_2 N'_2(i\omega) \quad , \quad (6.49)$$

where

$$k_1 = \frac{qD_n}{L} \coth\left(\frac{x'}{L}\right) \quad , \quad (6.50)$$

$$k_2 = \frac{qD_n}{L} \coth\left(\frac{W - x'}{L}\right) \quad . \quad (6.51)$$

There are also direct return currents  $i'_{r1}(t)$  and  $i'_{r2}(t)$  between  $x'$  and  $x' + \ell_f$ , as shown in Fig. 6.5. The Fourier-transformed return currents at  $x = x'$  and  $x = x' + \ell_f$  are identical and are expressed by

$$I'_{r1}(i\omega) = I'_{r2}(i\omega) = -\frac{qD_n}{\ell_f} [N'_1(i\omega) - N'_2(i\omega)] \quad . \quad (6.52)$$

Since there can be no accumulation of charge at any point in the entire  $p^+$ -layer, one must have current continuity at  $x = x'$  and  $x = x' + \ell_f$ :

$$I'_1(i\omega) + I'_{r1}(i\omega) + q = 0 \quad , \quad (6.53)$$

$$I'_2(i\omega) + I'_{r2}(i\omega) + q = 0 \quad . \quad (6.54)$$

From Eqs. (6.53) and (6.54), one obtains

$$N'_1(i\omega) = \frac{\ell_f}{D_n} \frac{k_1}{k_1 + k_2} \quad , \quad (6.55)$$

$$N'_2(i\omega) = -\frac{\ell_f}{D_n} \frac{k_2}{k_1 + k_2} \quad . \quad (6.56)$$

The Fourier-transformed electron density deviation  $N'(i\omega)$  calculated by Eq. (6.46) with the boundary conditions Eqs. (6.55) and (6.56) is plotted in Fig. 6.5. The circuit current

which actually flows in the external circuit is determined by the two relaxation currents  $I'_0(i\omega)$  at  $x = 0$  and  $I'_W(i\omega)$  at  $x = W$ :

$$I'_T(i\omega) = I'_0(i\omega) - I'_W(i\omega), \quad (6.57)$$

where

$$I'_0(i\omega) = qD_n \frac{\partial}{\partial x} N'(i\omega) \Big|_{x=0} = \frac{\ell_f}{D_n} \frac{k_0 k_2}{k_1 + k_2}, \quad (6.58)$$

$$I'_W(i\omega) = qD_n \frac{\partial}{\partial x} N'(i\omega) \Big|_{x=W} = \frac{\ell_f}{D_n} \frac{k_W k_1}{k_1 + k_2}, \quad (6.59)$$

$$k_0 = \frac{qD_n}{L_n} \operatorname{cosech} \left( \frac{x'}{L} \right), \quad (6.60)$$

$$k_W = \frac{qD_n}{L_n} \operatorname{cosech} \left( \frac{W - x'}{L} \right). \quad (6.61)$$

The reason why the total external circuit current  $I'_T(i\omega)$  is given by the difference of the two relaxation currents  $I'_0(i\omega)$  and  $I'_W(i\omega)$ , rather than the sum of two, is that this difference creates the departure from the charge neutrality in the entire  $p^+$ -region  $[0, W]$ . This should be compensated for by the external circuit current flow, which consists of the electron flow across the depletion layer and the hole flow across the  $p$ -type metal contact, in order to restore the charge neutrality. The external circuit current at the edge of junction  $x = 0$  is actually carried by many events of forward and backward electron thermionic emission and can be considered a continuous charging process just as the hole injection at  $x = W$ .

Equation (6.57) is the Fourier transform of the circuit current pulse due to a single-electron event in the  $p^+$ -layer. The average number of thermal diffusive transit events per second in a small volume  $A\Delta x$  (where  $A$  is the cross-section and  $\Delta x$  is the small distance along  $x$ ) is given by

$$\gamma_T = \frac{n(x)A\Delta x}{\bar{\tau}_f}. \quad (6.62)$$

Here  $\bar{\tau}_f$  is a mean-free time of the electron in the  $p^+$ -region. Since each thermal diffusive event occurs independently, the current fluctuation power spectral density due to such a random pulse train generated in this small volume is calculated using the Carson theorem:

$$\begin{aligned} \Delta S_{I'_T}(\omega) &= 2\gamma_T \overline{|I'_T(i\omega)|^2} \\ &= \frac{2n(x)A\Delta x}{\bar{\tau}_f} \frac{\overline{\ell_f^2}}{D_n^2} \left| \frac{k_0 k_2 - k_W k_1}{k_1 + k_2} \right|^2 \\ &= \frac{4A}{D_n} n(x) \left| \frac{k_0 k_2 - k_W k_1}{k_1 + k_2} \right|^2 \Delta x. \end{aligned} \quad (6.63)$$

Here,  $\overline{\ell_f^2} = 2D_n \bar{\tau}_f$  is used. The total current fluctuation power spectral density is given by integrating this equation in the entire  $p^+$ -layer:

$$\begin{aligned} S_{I'_T}(\omega) &= \frac{4A}{D_n} \int_0^W n(x) \left| \frac{k_0 k_2 - k_W k_1}{k_1 + k_2} \right|^2 dx \\ &\simeq \frac{4Aq^2 D_n}{L_n} \left( \frac{n_p - n_{p0}}{3} + \frac{n_{p0}}{2} \right). \end{aligned} \quad (6.64)$$

The second equality in the above expression is derived by assuming  $W \gg L_n$  and  $\omega\tau_n \ll 1$ ; that is, the above expression is valid only for a long diode and a low-frequency fluctuation component.

### 6.2.3 Generation-Recombination Noise

The initial action of this process is the instantaneous appearance or disappearance of an electron. If an electron is generated at  $x = x'$ , an instantaneous current  $-q\delta(t)$  flows from nowhere to  $x = x'$ , as shown in Fig. 6.6.

Solving the Fourier-transformed diffusion Eq. (6.46) for the boundary conditions  $N''(i\omega) = 0$  at  $x = 0$  and  $x = W$  and  $N''(i\omega) = N_1''$  at  $x = x'$ , one obtains

$$N''(i\omega) = \begin{cases} \frac{N_1''}{e^{x/L} - e^{-x'/L}} (e^{x/L} - e^{-x/L}) & (0 \leq x \leq x') \\ \frac{N_1''}{e^{(W-x')/L} - e^{-(W-x)/L}} [e^{(W-x)/L} - e^{-(W-x)/L}] & (x' \leq x \leq W) \end{cases} \quad (6.65)$$

The counter-propagating relaxation currents  $I_1''(i\omega)$  and  $I_2''(i\omega)$  at  $x = x'$  are now obtained

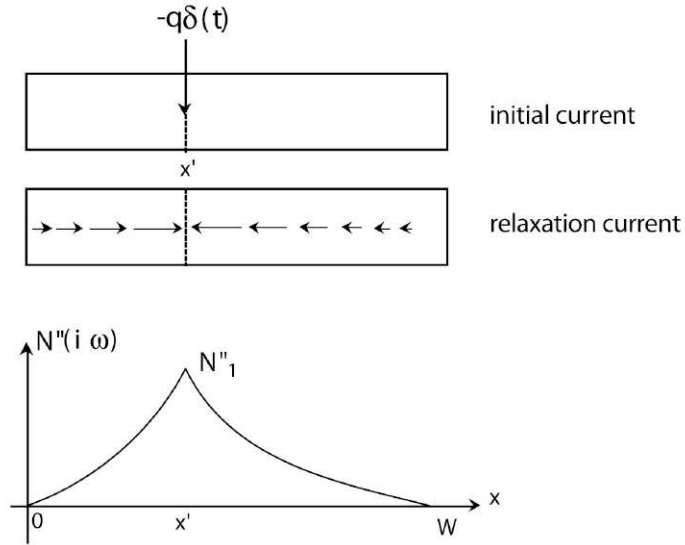


Figure 6.6: The initial current and subsequent relaxation current for a generation process of a minority carrier.

as,

$$I_1''(i\omega) = qD_n \left. \frac{\partial N''(i\omega)}{\partial x} \right|_{x=x'-0} = k_1 N_1''(i\omega) \quad , \quad (6.66)$$

$$I_2''(i\omega) = qD_n \left. \frac{\partial N''(i\omega)}{\partial x} \right|_{x=x'+0} = -k_2 N_1''(i\omega) \quad . \quad (6.67)$$

The current continuity at  $x = x'$  imposes the following relation:

$$I_1''(i\omega) - I_2''(i\omega) - q = 0 \quad . \quad (6.68)$$

From this condition, one can determine the value of  $N_1''(i\omega)$  as

$$N_1''(i\omega) = \frac{q}{k_1 + k_2} \quad . \quad (6.69)$$

The Fourier-transformed electron density deviation is plotted in Fig. 6.6. The relaxation currents at  $x = 0$  and  $x = W$  are given by

$$I_0''(i\omega) = qD_n \left. \frac{\partial N''(i\omega)}{\partial x} \right|_{x=0} = q \frac{k_0}{k_1 + k_2} \quad , \quad (6.70)$$

$$I_W''(i\omega) = qD_n \left. \frac{\partial N''(i\omega)}{\partial x} \right|_{x=W} = -q \frac{k_W}{k_1 + k_2} \quad . \quad (6.71)$$

The external circuit current is again given by the difference between Eqs. (6.70) and (6.71):

$$I_T''(i\omega) = q \left( \frac{k_0 + k_W}{k_1 + k_2} \right) \quad . \quad (6.72)$$

The average number of recombination events in a small volume  $A\Delta x$  is given by

$$\gamma_R = \frac{n(x)A\Delta x}{\tau_n} \quad , \quad (6.73)$$

while the average number of generation events is

$$\gamma_G = \frac{n_{p0}A\Delta x}{\tau_n} \quad . \quad (6.74)$$

Under the zero bias condition  $n(x) = n_{p0}$ , the recombination rate is equal to the generation rate, as it should be in a thermal equilibrium condition. This is called detailed balance. The current fluctuation power spectral density due to the generation and recombination events in this small volume is

$$\begin{aligned} \Delta S_{I_T''}(\omega) &= 2(\gamma_G + \gamma_R) \overline{|I_T''(i\omega)|^2} \\ &= 2 \frac{[n(x') + n_{p0}]A\Delta x}{\tau_n} q^2 \left| \frac{k_0 + k_W}{k_1 + k_2} \right|^2 \quad . \end{aligned} \quad (6.75)$$

The total current fluctuation power spectral density is calculated by integrating (6.75) from  $x = 0$  to  $x = W$ :

$$\begin{aligned} S_{I_T''}(\omega) &= \frac{2Aq^2}{\tau_n} \int_0^W [n(x') + n_{p0}] \left| \frac{k_0 + k_W}{k_1 + k_2} \right|^2 dx' \\ &\simeq \frac{2Aq^2 D_n}{L_n} \left[ \frac{n_p - n_{p0}}{3} + n_{p0} \right] \quad , \end{aligned} \quad (6.76)$$

where  $W \gg L_n$  (long-diode limit) and  $\omega\tau_n \ll 1$  (low-frequency limit) are used to derive the second equality.

### 6.2.4 Total Current Noise

The total current fluctuation power spectral density is the simple sum of Eqs. (6.64) and (6.76)

$$S_{I_T}(\omega) = \underbrace{\frac{4Aq^2 D_n}{L_n} \left( \frac{n_p - n_{p0}}{3} + \frac{n_{p0}}{2} \right)}_{\text{Thermal Diffusion Noise}} + \underbrace{\frac{4Aq^2 D_n}{L_n} \left( \frac{n_p - n_{p0}}{6} + \frac{n_{p0}}{2} \right)}_{\text{Generation - Recombination Noise}} . \quad (6.77)$$

The following three bias regions feature different noise characteristics:

(1) Zero Bias ( $V = 0$ )

In this case,  $n_p = n_{p0}$ , and thus Eq. (6.77) is simplified to

$$S_{I_T}(\omega) = \frac{4Aq^2 D_n n_{p0}}{L_n} = \frac{4k_B \theta}{R_d(V=0)} , \quad (6.78)$$

where  $R_d(V=0) = \frac{L_n k_B \theta}{Aq^2 D_n n_{p0}}$  is the differential resistance  $\left(\frac{dI}{dV}\right)^{-1}$  at  $V=0$ . Equation (6.78) is the Johnson-Nyquist thermal noise. This result is expected because the junction is in thermal equilibrium at  $V=0$  and thus the Johnson-Nyquist formula should be applied.

However, note that only one-half of Eq. (6.78) stems from standard thermal diffusion noise and the remaining half is due to generation-recombination noise. In this sense, a simple microscopic theory of a thermal diffusion process for a metallic conductor cannot describe the thermal equilibrium noise of a  $pn$  junction. On the other hand, the Nyquist approach to thermal noise is very general; it does not depend on the detailed microscopic process in a resistive element, but only requires the resistive element be in thermal equilibrium with the environments. There are two “environments” for a  $pn$  junction: lattice vibration (thermal phonon reservoirs) which are responsible for thermal diffusion noise and electromagnetic field (thermal photon reservoirs) which are responsible for generation-recombination noise. The Johnson-Nyquist formula holds due to the equal contribution by phonon reservoirs and photon reservoirs.

(2) Forward Bias ( $V > 0$ )

Equation (6.77), in this case, is reduced to

$$S_{I_T}(\omega) = \frac{2Aq^2 D_n}{L_n} (n_p + n_{p0}) = 2q(I + 2I_s) , \quad (6.79)$$

where the forward current  $I$  and the (reverse) saturation current  $I_s$  are given by

$$I = \frac{AqD_n}{L_n} (n_p - n_{p0}) , \quad (6.80)$$

$$I_s = \frac{AqD_n}{L_n} n_{p0} . \quad (6.81)$$

In a reasonably high forward bias voltage, Eq. (6.79) is reduced to the full-shot noise  $2qI$  since  $I \gg I_s$ . Two-thirds of the full-shot noise is due to thermal diffusion noise and one-third is due to generation-recombination noise. The generation-recombination noise in this case is dominated by the radiative recombination (spontaneous emission) noise for a direct bandgap semiconductor. In this way, we can conclude that two-thirds of the shot noise of a forward-biased  $pn$  junction is thermal noise and one-third is quantum noise.

### (3) Reverse Bias ( $V < 0$ )

In this case  $n_p \ll n_{p0}$ , and thus Eq. (6.77) becomes

$$S_{I_T}(\omega) = \frac{2Aq^2D_n}{L_n}n_{p0} = 2qI_s \quad . \quad (6.82)$$

This result is often referred to as a “dark current shot noise,” which is the dominant noise source of a reverse-biased photodiode and avalanche photodiode. In this case, one-third of the full-shot noise is due to thermal diffusion noise and two-thirds is due to generation-recombination noise. The generation-recombination noise in this case is dominated by the absorption of thermal photons. Thus, we can conclude that the full shot noise of a reverse-biased  $pn$  junction is solely due to thermal noise.

## 6.2.5 Short Diode

Thus far a so-called long diode with a bulk  $p^+$ -layer thickness  $W$  much longer than the diffusion length  $L_n$  has been studied. However, some  $pn$  junction diodes, such as a double-heterostructure semiconductor laser diode and heterojunction bipolar transistor, have a much thinner  $p^+$ -layer than the electron diffusion length ( $W \ll L_n$ ).

Consider a  $N$ - $p^+$ - $P$  double-heterostructure diode, as shown in Fig. 6.7. An injected electron from the  $N$ -layer to the  $p^+$ -layer cannot diffuse freely toward the  $p$ -side metal contact due to the conduction band discontinuity at the  $p^+$ - $P$  isotype heterojunction. A junction current is not carried by a thermal diffusion process, but crosses an “imaginary plane” between the conduction and valence bands by a “recombination process.” The electron and hole densities are uniform in the  $p^+$ -layer since  $W \ll L_n$ . The electron density in a relatively small bias voltage is given by[4]

$$n_p = n_{p0} \exp\left(\frac{V}{V_T}\right) \quad . \quad (6.83)$$

The junction current is related to the total electron number in the  $p^+$ -layer,  $N_e \equiv AWn$ , by

$$I = q \frac{N_e}{\tau_n} \quad . \quad (6.84)$$

The differential resistance  $R_d$  and diffusion capacitance  $C_{dif}$  are given by

$$R_d \equiv \left(\frac{dI}{dV}\right)^{-1} = \frac{V_T\tau_n}{qN_e} \quad , \quad (6.85)$$

$$C_{dif} \equiv \frac{dQ_{(\text{minority carrier})}}{dV} = \frac{qN_e}{V_T} \quad . \quad (6.86)$$

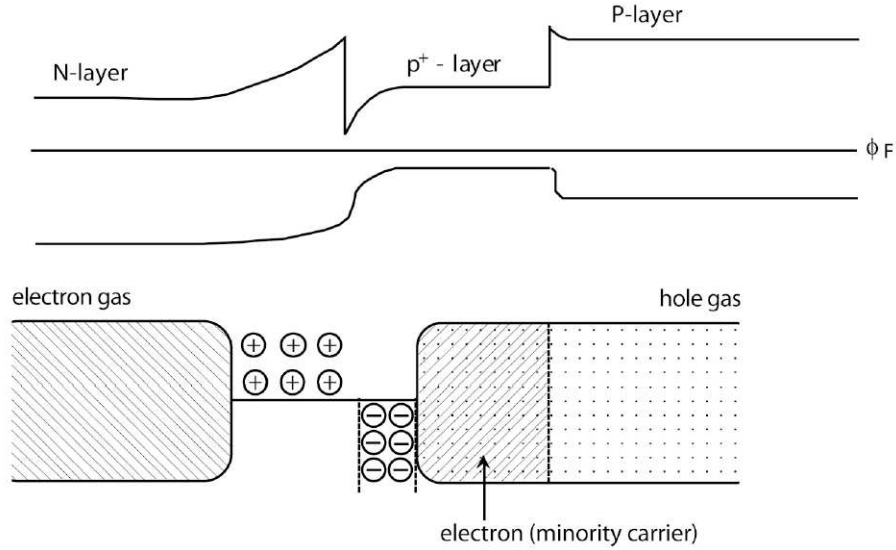


Figure 6.7: A  $N$ - $p^+$ - $P$  double heterostructure diode.

The depletion layer capacitance  $C_{dep}$  is still given by Eq. (6.45).

Next, the current-fluctuation power spectral density due to thermal diffusion noise and generation-recombination noise will be calculated. When  $W \ll L_n$ , one obtains

$$\frac{k_0 k_2}{k_1 + k_2} \simeq \frac{k_W k_1}{k_1 + k_2} \simeq \frac{q D_n}{W} \quad , \quad (6.87)$$

and from Eqs. (6.58) and (6.59),

$$I'_0(i\omega) \simeq I'_W(i\omega) = \frac{q \ell_f}{W} \quad . \quad (6.88)$$

At each boundary there is a fluctuating current with the power spectral density

$$\begin{aligned} S_{I'_0}(\omega) = S_{I'_W}(\omega) &= \int_0^W \frac{2n_p A}{\bar{\tau}_f} \overline{\left(\frac{q \ell_f}{W}\right)^2} dx \\ &= 4qI \left(\frac{L_n}{W}\right)^2 \quad , \end{aligned} \quad (6.89)$$

where  $D_n = \overline{\ell_f^2} / 2\bar{\tau}_f = L_n^2 / \tau_n$  is used. This current noise is much larger than the full-shot noise since  $L_n/W \gg 1$ . However, as indicated in Eq. (6.88), the fluctuating currents  $I'_0(i\omega)$  and  $I'_W(i\omega)$  are identical, *i.e.* positively correlated, and thus cancel out completely to nullify the total external circuit current fluctuation,

$$I'_T(i\omega) = I'_0(i\omega) - I'_W(i\omega) = 0 \quad . \quad (6.90)$$

The thermal diffusion noise does not produce any departure from the charge neutrality in the  $p^+$ -region  $[0, W]$  and thus does not induce any external circuit current noise.

When  $W \ll L_n$ , one obtains

$$\frac{k_0}{k_1 + k_2} \simeq 1 - \frac{x'}{W} \quad , \quad (6.91)$$

$$\frac{k_W}{k_1 + k_2} \simeq \frac{x'}{W} \quad . \quad (6.92)$$

Using these relations in Eqs. (6.70) and (6.71), one obtains

$$I_0''(i\omega) = q \left( 1 - \frac{x'}{W} \right) \quad , \quad (6.93)$$

$$I_W''(i\omega) = -q \frac{x'}{W} \quad , \quad (6.94)$$

$$I_T''(i\omega) = I_0''(i\omega) - I_W''(i\omega) = q \quad . \quad (6.95)$$

Each event of electron generation and recombination results in independent current pulses with a time-integrated area equal to  $q$  in the external circuit and thus the low-frequency power spectral density is given by the sum of the two contributions,

$$S_{I_T}''(\omega) = 2q^2(N_e + N_{e0})/\tau_n \quad . \quad (6.96)$$

This expression is reduced to the Johnson-Nyquist formula of thermal noise at  $V = 0$  and the Schottky formula of full-shot noise at  $V > 0$  or  $V < 0$ :

(1) Zero-Bias ( $V = 0$ )

$$S_{I_T}''(\omega) = \frac{4q^2 N_{e0}}{\tau_n} = \frac{4k_B\theta}{R_d(V=0)} \quad . \quad (6.97)$$

A  $pn$  junction is in equilibrium with thermal photon reservoir. One half of this thermal noise is to thermal photon absorption and the remaining half is contributed by radiative recombination (spontaneous emission).

(2) Forward-Bias ( $V > 0$ )

$$S_{I_T}''(\omega) = 2q^2 \frac{N_c}{\tau_n} = 2qI \quad . \quad (6.98)$$

This full-shot noise is due solely to the radiative recombination (spontaneous emission) process, so it has a quantum mechanical origin.

(3) Reverse-Bias ( $V < 0$ )

$$S_{I_T}''(\omega) = 2q^2 \frac{N_{c0}}{\tau_n} = 2qI_s \quad . \quad (6.99)$$

This full-shot noise is due solely to the generation (thermal photon absorption) process.

## 6.3 Bipolar Transistor

The bipolar transistor (transfer resistor) is one of the most important semiconductor devices and is now widely used in high speed computer and communication systems. The noise figure of a bipolar transistor is determined by the shot noise of a  $pn$  junction diode biased by a constant voltage source discussed above. We will study the basic noise properties of a bipolar transistor in this section.

### 6.3.1 Current-Voltage Relationship

The basic structure of a p-n-p bipolar transistor is shown in Fig. 6.8(a), which consists of a forward-biased emitter junction and reverse-biased collector junction. A bipolar transistor is usually used in two different circuit configurations. Figure 6.8(b) and (c) show the common base configuration and common emitter configurations for a p-n-p bipolar transistor.

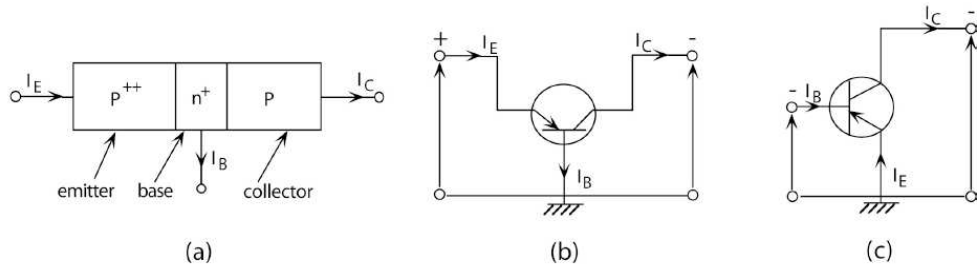


Figure 6.8: The basic structure (a) and two circuit configurations of common-base (b) and common emitter (c) for a p-n-p bipolar transistor.

Consider the p-n-p bipolar transistor with uniform doping profile and in a common base configuration (Fig. 6.9). The continuity and current density equations in the neutral base region are given by[4]

$$0 = -\frac{p - p_B}{\tau_B} + D_B \frac{\partial^2 p}{\partial x^2} \quad , \quad (6.100)$$

$$J_p = -qD_B \frac{\partial p}{\partial x} \quad , \quad (6.101)$$

$$J_n = J_{tot} + qD_B \frac{\partial p}{\partial x} \quad . \quad (6.102)$$

The excess minority carrier densities at the edge of the emitter-base depletion layer are

$$p'(0) \equiv p(0) - p_B = p_B \left[ \exp\left(\frac{qV_{EB}}{k_B T}\right) - 1 \right] \quad , \quad (6.103)$$

$$n'(-x_E) \equiv n(-x_E) - n_E = n_E \left[ \exp\left(\frac{qV_{EB}}{k_B T}\right) - 1 \right] \quad . \quad (6.104)$$

A similar set of equations can be found for the collector-base junction:

$$p'(W) \equiv p(W) - p_B = p_B \left[ \exp\left(\frac{qV_{CB}}{k_B T}\right) - 1 \right] , \quad (6.105)$$

$$n'(x_C) \equiv n(x_C) - n_C = n_C \left[ \exp\left(\frac{qV_{CB}}{k_B T}\right) - 1 \right] . \quad (6.106)$$

The solutions for the minority carrier distributions in the base, emitter and collector regions are easily obtained,

$$p(x) = p_B + \left[ \frac{p'(W) - p'(0)e^{-W/L_B}}{2 \sinh(W/L_B)} \right] e^{x/L_B} - \left[ \frac{p'(W) - p'(0)e^{W/L_B}}{2 \sinh(W/L_B)} \right] e^{-x/L_B} , \quad (6.107)$$

$$n(x) = n_E + n'(-x_E) \exp\left(\frac{x + x_E}{L_E}\right) , \quad (6.108)$$

$$n(x) = n_C + n'(x_C) \exp\left(-\frac{x - x_C}{L_C}\right) . \quad (6.109)$$

From Eqs. (6.101) and (6.102) we can obtain the total dc emitter current:

$$\begin{aligned} I_E &= A J_p(x=0) + A J_n(x=-x_E) \\ &= A \left( -qD_B \frac{\partial p}{\partial x} \Big|_{x=0} \right) + A \left( -qD_E \frac{\partial n}{\partial x} \Big|_{x=-x_E} \right) \\ &= Aq \frac{D_B p_B}{L_B} \coth\left(\frac{W}{L_B}\right) \left[ \left( e^{qV_{EB}/k_B T} - 1 \right) - \frac{1}{\cosh(W/L_B)} \left( e^{qV_{CB}/k_B T} - 1 \right) \right] \\ &\quad + Aq \frac{D_E n_E}{L_E} \left( e^{qV_{EB}/k_B T} - 1 \right) . \end{aligned} \quad (6.110)$$

Similarly we can obtain the total dc collector current:

$$\begin{aligned} I_C &= A J_p(x=W) + A J_n(x=x_C) \\ &= A \left( -qD_B \frac{\partial p}{\partial x} \Big|_{x=W} \right) + A \left( -qD_C \frac{\partial n}{\partial x} \Big|_{x=x_C} \right) \\ &= Aq \frac{D_B p_B}{L_B} \cdot \frac{1}{\sinh(W/L_B)} \left[ \left( e^{qV_{EB}/k_B T} - 1 \right) - \cosh\left(\frac{W}{L_B}\right) \left( e^{qV_{CB}/k_B T} - 1 \right) \right] \\ &\quad + Aq \frac{D_C n_C}{L_C} \left( e^{qV_{CB}/k_B T} - 1 \right) . \end{aligned} \quad (6.111)$$

Here  $A$  is the cross-sectional area of the transistor. The difference between these two currents appears as the base current:

$$I_B = I_E - I_C . \quad (6.112)$$

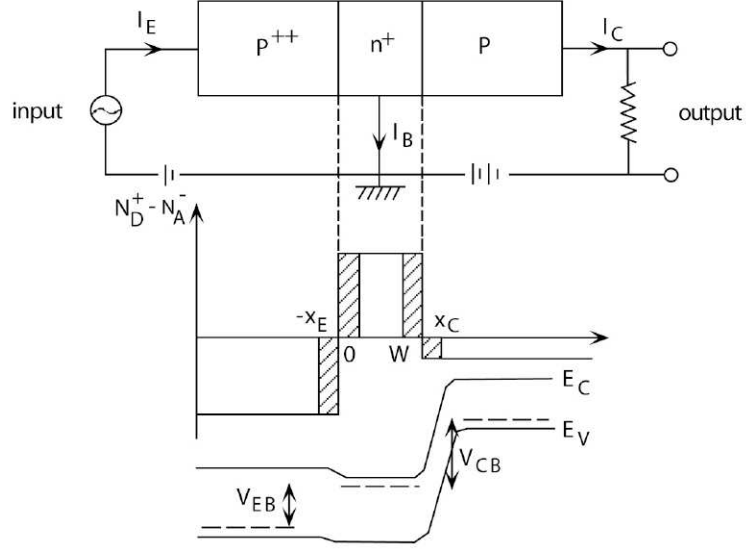


Figure 6.9: The common-base configuration, doping profile and band diagram of the p-n-p bipolar transistor.

### 6.3.2 Current Gain

The common-base current gain  $\alpha_0$ , often represented by  $h_{FB}$ , is defined as

$$\alpha_0 = \frac{\partial I_C}{\partial I_E} = \frac{\partial I_{PE}}{\partial I_E} \frac{\partial I_{PC}}{\partial I_{PE}} \frac{\partial I_C}{\partial I_{PC}} \quad , \quad (6.113)$$

where  $I_{PE}$  and  $I_{PC}$  are the emitter and collector currents carried by holes, *i.e.* the first term of Eqs. (6.110) and (6.111). The first term  $\frac{\partial I_{PE}}{\partial I_E}$  is called as the emitter efficiency  $\gamma$ , the second term  $\frac{\partial I_{PC}}{\partial I_{PE}}$  the base transport factor  $\alpha_T$ , and the third term  $\frac{\partial I_C}{\partial I_{PC}}$  the collector multiplication factor  $M$ . Since the transistor is normally operated well below the avalanche breakdown voltage for a base-collector junction, the multiplication factor is  $M \simeq 1$  and so the static common-base current gain is given by

$$\alpha_0 \simeq \gamma \alpha_T \quad . \quad (6.114)$$

On the other hand, the static common-emitter current gain  $\beta_0$ , often represented by  $h_{FE}$ , is defined as

$$\beta_0 = \frac{\partial I_C}{\partial I_B} = \frac{\alpha_0}{1 - \alpha_0} \quad , \quad (6.115)$$

where we used Eq. (6.112).

Under the normal operating condition of a p-n-p bipolar transistor,  $V_{EB} > 0$  and  $V_{CB} \ll 0$ , so the terms in Eqs. (6.110) and (6.111) associated with  $V_{CB}$  can be neglected compared to the reverse-bias saturation current. The emitter efficiency  $\gamma$  is calculated from Eq. (6.110) as

$$\gamma = \frac{\partial A J_P(x=0)}{\partial I_E} = \left[ 1 + \frac{n_E D_E L_B}{p_B D_B L_E} \tanh\left(\frac{W}{L_B}\right) \right]^{-1} \quad . \quad (6.116)$$

The base transport factor  $\alpha_T$  is obtained from Eqs. (6.110) and (6.111) as

$$\alpha_T = \frac{J_P(x=W)}{J_P(x=0)} = \frac{1}{\cosh(W/L_B)} \quad . \quad (6.117)$$

For bipolar transistors with base width much smaller than the diffusion length,  $\alpha_T$  is close to one, and the current gain is determined solely by the emitter efficiency. Under this condition,

$$\beta_0 = \frac{\gamma}{1-\gamma} = \frac{p_B D_B L_E}{n_E D_E L_B} \coth\left(\frac{W}{L_B}\right) \quad . \quad (6.118)$$

For a given emitter doping level  $p_E$ , the current gain  $\beta_0$  increases with decreasing the base doping level  $n_B$ .

### 6.3.3 Input vs. Output Characteristics

For a bipolar transistor with high emitter efficiency, the dc emitter and collector currents, Eqs. (6.110) and (6.111), reduce to the hole currents, *i.e.* the terms proportional to  $\frac{\partial p}{\partial x}$  at  $x=0$  and  $x=W$ , respectively. That is, the emitter and collector currents are determined by the hole density gradients at the edges of the base region. The base current is given by the difference between the emitter and collector currents.

Figure 6.10(a) shows the input-output characteristics of the common-base configuration. The collector current is practically equal to the emitter current, *i.e.*  $\alpha_0 \simeq 1$  and is independent of  $V_{CB}$ . This means  $\frac{\partial p}{\partial x}$  at  $x=0$  is equal to  $\frac{\partial p}{\partial x}$  at  $x=W$  for varying  $V_{EB}$  and  $V_{CB}$ , as shown in Fig. 6.11(a) and (b). To reduce the collector current to zero, a forward bias voltage must be applied to the collector, where the hole density at  $x=W$  becomes equal to the hole density at  $x=0$ , as shown in Fig. 6.11(c). The collector saturation current  $I_{CO}$  (Fig. 6.10(a)) with the emitter circuit open ( $I_E=0$ ) is considerably smaller than the ordinary reverse bias current of a p-n junction, because  $\frac{\partial p}{\partial x}=0$  at  $x=0$ , which results in the reduction of  $\frac{\partial p}{\partial x}$  at  $x=W$  as shown in Fig. 6.11(d). At a sufficiently strong bias voltage  $V_{CB}$ , the collector current starts to increase rapidly (Fig. 6.10(a)). This is either by the avalanche breakdown effect or the punch-through effect. In the latter case the collector depletion region reaches the emitter depletion region and a large direct current flows from the emitter to the collector.

Figure 6.10(b) shows the input-output characteristics of the common-emitter configuration. The current gain in this case is much greater than one ( $\beta_0 \gg 1$ ). The saturation current  $I'_{CO}$  with the base circuit open ( $I_B=0$ ) is much larger than ( $I_{CO}$ ), since

$$I_B = I_E - I_C = I_E - (I_{CO} + \alpha_0 I_E) \quad , \quad (6.119)$$

and therefore

$$I'_{CO} = I_C(I_B=0) = \frac{I_{CO}}{1-\alpha_0} \gg I_{CO} \quad . \quad (6.120)$$

As  $V_{CE}$  increases, the base width decreases and the current gain  $\beta_0$  increases. The lack of saturation in the common-emitter output characteristics is called Early effect[4]. When  $V_{CE}$  decreases with a constant  $I_B$ , the collector junction is eventually forward-biased and the collector current becomes zero (Fig. 6.10(c)).

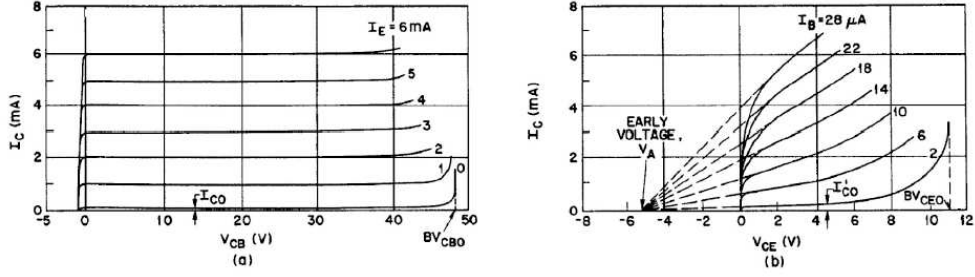


Figure 6.10: Input-output characteristics for a p-n-p transistor in (a) common-base configuration and (b) common-emitter configuration.

### 6.3.4 Current Noise

In the absence of emitter-base and collector-base depletion-layer recombination processes, the current-voltage characteristics at the two junctions are governed by Schockley's diffusion theory of a pn junction. The bipolar transistor is called ideal in such a case. If the emitter and collector currents are carried only by holes, the emitter and collector current noise spectral densities are obtained from the analyses presented in the previous section and written as

$$S_{i_E}(\omega) = \frac{4A}{D} I_1 + \frac{2q^2 A}{\tau_R} I_2 \quad , \quad (6.121)$$

$$S_{i_C}(\omega) = \frac{4A}{D} I_3 + \frac{2q^2 A}{\tau_R} I_4 \quad , \quad (6.122)$$

where the first terms in Eqs. (6.22) and (6.122) represent the thermal diffusion noise of minority carriers, holes, in the base region, and the second terms in Eqs. (6.22) and (6.122) represent the generation-recombination noise in the base region. The integrals  $I_j$  ( $j = 1$  to 4) take the same forms as those derived in the previous section:

$$I_1 = \int_0^W p \left| \frac{k_0 k_2}{k_1 + k_2} \right|^2 dx \quad , \quad (6.123)$$

$$I_2 = \int_0^W (p + p_n) \left| \frac{k_0}{k_1 + k_2} \right|^2 dx \quad , \quad (6.124)$$

$$I_3 = \int_0^W p \left| \frac{k_1 k_W}{k_1 + k_2} \right|^2 dx \quad , \quad (6.125)$$

$$I_4 = \int_0^W (p + p_n) \left| \frac{k_W}{k_1 + k_2} \right|^2 dx \quad . \quad (6.126)$$

By evaluating the integrals Eqs. (6.123)-(6.126), the spectral densities Eqs. (6.22) and (6.122) reduce to the forms,

$$S_{i_E}(\omega) = 4qI_E \left( \frac{G_E}{G_{EO}} - \frac{1}{2} \right) \quad , \quad (6.127)$$

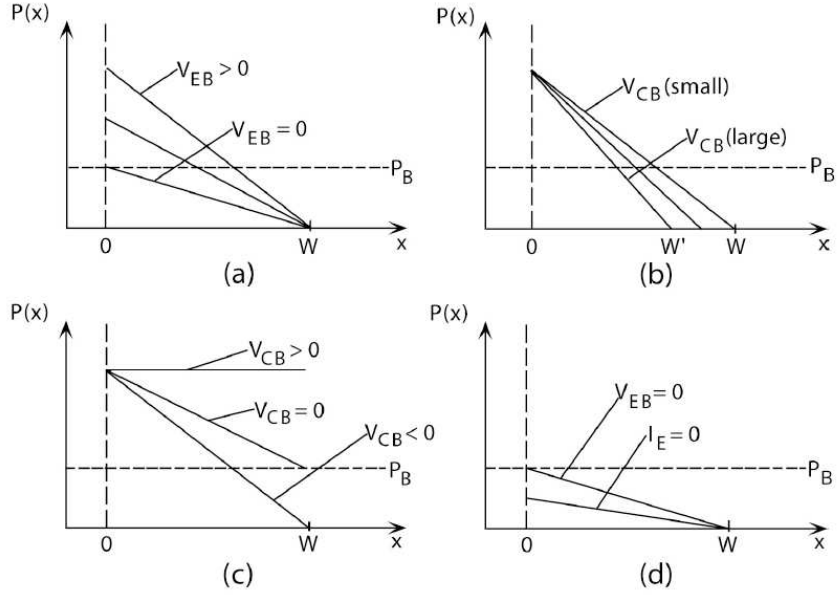


Figure 6.11: Hole density in the base region of a p-n-p bipolar transistor. (a)  $V_{CB} = \text{constant}$  and  $V_{EB}$  varying. (b)  $V_{EB} = \text{constant}$  and  $V_{CB}$  varying. (c)  $V_{CB} = \text{forward, zero and reverse biased}$ . (d) zero emitter current and zero emitter voltage.

$$S_{i_C}(\omega) = 2qI_C \quad . \quad (6.128)$$

Here  $G_E$  is the conductance of the forward-biased emitter-base junction and  $G_{EO}$  is the low frequency value of  $G_E$ . At low frequencies,  $G_E \simeq G_{EO}$  and the forward-biased emitter current shows full shot noise. The reverse-biased collector current features full shot noise at all frequencies.

Since the same noise generation mechanisms are responsible for the emitter and collector current noise, some degree of correlation should be expected between the two fluctuations. When either thermal diffusion or generation-recombination event occurs in the base region, the relaxation current pulses,  $f_E(t)$  and  $f_C(t)$ , flow in the two junctions. The cross-spectral density between  $i_E$  and  $i_C$  is given by the extended Carson theorem:

$$S_{CE}(\omega) = 2\nu a^2 F_E(i\omega) F_C(i\omega)^* \quad , \quad (6.129)$$

where  $\nu$  is the mean rate of the pulse emission,  $a (= q)$  is the pulse area and  $F_E(i\omega)$  and  $F_C(i\omega)$  are the Fourier transform of the relaxation current pulse shape functions  $f_E(t)$  and  $f_C(t)$ . Using the expressions for the two-types of noise currents of the previous section, Eq. (6.129) reduces to the form

$$S_{CE}(\omega) = \frac{4A}{D} I_5 - \frac{2q^2 A}{\tau_R} I_6 \quad , \quad (6.130)$$

where

$$I_5 = \int_0^W p \frac{k_1 k_W k_0^* k_2^*}{|k_1 + k_2|^2} dx \quad , \quad (6.131)$$

$$I_6 = \int_0^W (p + p_n) \frac{k_0^* k_W}{|k_1 + k_2|^2} dx \quad . \quad (6.132)$$

By evaluating the integrals in Eqs. (6.131) and (6.132), the cross-spectral density is expressed as

$$S_{CE}(\omega) = 2qI_C \frac{\alpha_0 Y_E}{\alpha_{00} G_{EO}} \quad , \quad (6.133)$$

where  $\alpha_0$  is the common-base current gain,  $\alpha_{00}$  is the low-frequency value of  $\alpha_0$ , and  $Y_E$  is the admittance of the emitter-base junction. For low frequencies,  $Y_E$  becomes equal to  $G_{EO}$  and Eq. (6.133) has the frequency independent form,

$$S_{CE}(\omega \simeq 0) = 2qI_C \quad . \quad (6.134)$$

The normalized cross-spectral density between the emitter and collector currents is defined as

$$\Gamma_{CE} \equiv \frac{S_{CE}(\omega)}{[S_{i_E}(\omega) S_{i_C}(\omega)]^{1/2}} \quad . \quad (6.135)$$

For low frequencies,  $S_{i_E}(\omega) = 2qI_E = 2qI_C/\alpha_{00}$  and hence

$$\Gamma_{CE} = \alpha_{00}^{1/2} \quad . \quad (6.136)$$

Since a modern bipolar transistor has  $\alpha_{00} \simeq 1$ , the fluctuations in the emitter and collector currents are highly and positively correlated.

The power spectrum of the fluctuations in the base current,  $I_B = I_E - I_C$ , is given by

$$\begin{aligned} S_{i_B}(\omega) &= S_{i_E}(\omega) + S_{i_C}(\omega) - 2\text{Re}[S_{CE}(\omega)] \\ &= 2qI_C \left[ \frac{1}{\beta_0} + \frac{2G_E - (\alpha_0 Y_E + \alpha_0^* Y_E^*)}{\alpha_{00} G_{EO}} - \frac{2(1 - \alpha_{00})}{\alpha_{00}} \right] \quad , \quad (6.137) \end{aligned}$$

where  $\beta_0 = I_C/I_B$  is the common-emitter current gain. At low frequencies,  $S_{i_B}(\omega)$  is reduced to  $2qI_B$ , which features the full shot noise.

The cross-spectral density between  $I_C$  and  $I_B$  is given by

$$\begin{aligned} S_{CB}(\omega) &= S_{CE}(\omega) - S_{i_C}(\omega) \\ &= -2qI_C \left[ 1 - \frac{\alpha_0 Y_E}{\alpha_{00} G_{EO}} \right] \quad . \quad (6.138) \end{aligned}$$

The term  $\alpha_0 Y_E$  is expanded to first order in frequency[3, 4]:

$$\alpha_0 Y_E \simeq \alpha_{00} G_{EO} \left( 1 - \frac{i\omega\tau_B}{3} \right) \quad , \quad (6.139)$$

where  $\tau_B = W^2/2D_B$  is the base-layer charging time. Using Eq. (6.139) in (6.138), the cross-spectral density and the normalized cross-spectral density are approximated by

$$S_{CB}(\omega) = -2qI_C \left( \frac{i\omega\tau_B}{3} \right) \quad , \quad (6.140)$$

$$\Gamma_{CB}(\omega) \equiv \frac{S_{CB}(\omega)}{[S_{i_C}(\omega) S_{i_B}(\omega)]^{1/2}} = -\beta_0^{1/2} \left( \frac{i\omega\tau_B}{3} \right) . \quad (6.141)$$

Similarly we obtain the cross-spectral density and the normalized cross-spectral density between the emitter and base currents:

$$\begin{aligned} S_{EB}(\omega) &= S_{i_E}(\omega) - S_{EC}(\omega) \\ &= -2qI_C \left[ \frac{2G_E}{\alpha_{00}G_{EO}} - \frac{2}{\alpha_{00}} + \frac{1}{\beta_0} + 1 - \frac{\alpha_0^* Y_E^*}{\alpha_{00}G_{EO}} \right] \\ &\simeq -2qI_C/\beta_0 \quad (\omega \simeq 0) , \end{aligned} \quad (6.142)$$

$$\Gamma_{EB} \equiv \frac{S_{EB}(\omega)}{[S_{i_E}(\omega) S_{i_B}(\omega)]^{1/2}} \simeq - \left( \frac{\alpha_0}{\beta_0} \right)^{1/2} \quad (\omega \simeq 0) . \quad (6.143)$$

### 6.3.5 Noise Figure

For small signal condition the bipolar transistor is essentially a linear device and it is represented by an equivalent circuit of a linear two-port, as shown in Fig. 6.12. The admittance matrix of the intrinsic transistor, in which the base resistance is neglected, is

$$Y = \begin{bmatrix} \frac{1}{r_{BE}} + \frac{1}{r_{BC}} + i\omega(C_{BE} + C_{BC}) & \frac{1}{r_{BC}} + i\omega C_{BC} \\ -g_m + \frac{1}{r_{BC}} + i\omega C_{BC} & \frac{1}{r_{BC}} + i\omega C_{BC} \end{bmatrix} , \quad (6.144)$$

where  $g_m = \frac{\partial I_C}{\partial V_{BE}}$  is the mutual conductance of the transistor,  $r_{BE} = \frac{\beta_{00}}{g_m}$  and  $C_{BE} = g_m\tau_B$ [4]. In a normal operating condition, the reverse-biased base-collector junction has the negligible admittance, that is,  $\frac{1}{r_{BC}} \ll \frac{1}{r_{BE}}$  and  $C_{BC} \ll C_{BE}$ . Therefore, the two non-zero components of admittance matrix reduce to  $Y_{11} \simeq g_m \left( \frac{1}{\beta_{00}} + i\omega\tau_B \right)$  and  $Y_{21} = -g_m$ , respectively.

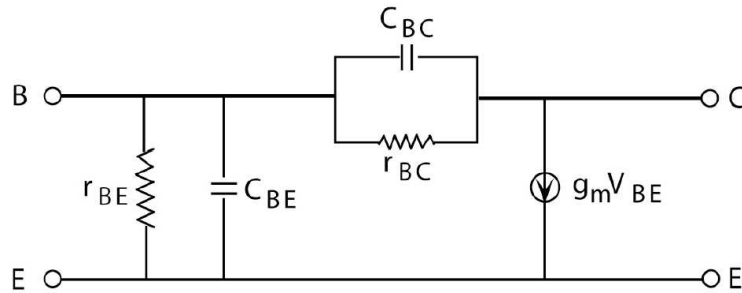


Figure 6.12: An equivalent circuit of the bipolar transistor.

The base current noise  $i_B$  and the collector current noise  $i_C$ , derived above, must be added as the external noise sources to the above noiseless equivalent circuit. This is shown in Fig. 6.13(a). The spectral densities and cross-spectral densities of these current noise are given by Eqs. (6.128), (6.137) and (6.140). For calculating the noise figure of the bipolar transistor of a common emitter configuration, it is convenient to transfer the output noise generator to the input. We obtain the two new noise generators  $i_{na}$  and  $v_{na}$

at the input, as shown in Fig. 6.13(b). This circuit is valid for calculating the output noise but not for calculating the input noise as discussed in Chapter 3. The Fourier transform of the new noise generators are

$$V_{na} = -\frac{I_C}{Y_{21}} \quad , \quad (6.145)$$

$$I_{na} = I_B - \frac{Y_{11}}{Y_{21}} I_C \quad , \quad (6.146)$$

where the  $Y$  parameters are given by Eq. (6.144). The spectral densities of the two generators are

$$S_{V_{na}}(\omega) \simeq 2qI_C/G_{EO}^2 \quad , \quad (6.147)$$

$$S_{I_{na}}(\omega) \simeq 2qI_B + \frac{4}{3}qI_C\omega^2\tau_B^2 \quad , \quad (6.148)$$

and the cross-spectral density between them is

$$S_{V_{na}I_{na}}(\omega) \simeq 2qI_C \left( \frac{1}{\beta_{00}} - \frac{2}{3}i\omega\tau_B \right) / G_{EO} \quad . \quad (6.149)$$

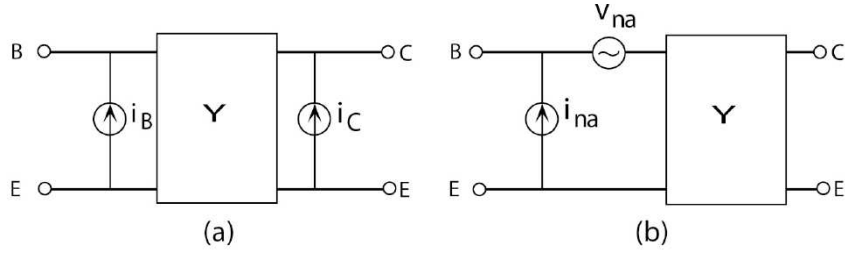


Figure 6.13: The noise equivalent circuits of the bipolar transistor.

The noise figure of the transistor is the ratio of total noise power at the output to the noise power resulting from thermal noise in source resistance and is calculated from the circuit shown in Fig. 6.14. Here  $i_s$  is the input signal current generator,  $Y_s = G_s + iB_s$  is the source admittance,  $i_{ns}$  is the source resistance thermal noise with spectral density equal to  $4k_B\theta G_s$ ,  $i_{nb}$  is the equivalent noise current generator to  $v_{na}$  in Fig. 6.13(b). The Fourier transform of this new noise current is (Chapter 13),

$$I_{nb} = Y_s V_{na} \quad . \quad (6.150)$$

The noise figure is calculated from Eqs. (6.147)-(6.149) as,

$$F = 1 + \frac{2qI_C}{4k_B T G_s} \left[ \left( \frac{B_s}{G_{EO}} + \frac{2}{3}\omega\tau_B \right)^2 + \frac{2}{9}\omega^2\tau_B^2 + \frac{1}{\beta_0} + \frac{G_s^2}{G_{EO}^2} + \frac{2G_s}{G_{EO}\beta_{00}} \right] \quad . \quad (6.151)$$

The noise tuning condition (Chapter 3) is satisfied when the source susceptance  $B_s$  is equal to

$$B_s = -\frac{2}{3}\omega\tau_B G_{EO} \quad . \quad (6.152)$$

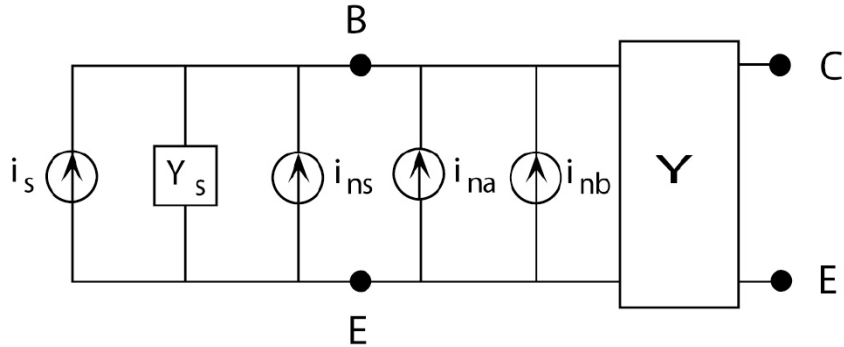


Figure 6.14: A noise equivalent circuit of the bipolar transistor including the source admittance  $Y_s$  and source resistance thermal noise current  $i_{ns}$ .

The optimum source conductance which minimizes the noise figure is obtained by the condition,  $\frac{\partial F}{\partial G_s} = 0$ , and is given by

$$G_s = G_{EO} \left( \frac{1}{\beta_0} + \frac{2}{9} \omega^2 \tau_B^2 \right)^{1/2} . \quad (6.153)$$

If we substitute Eqs. (6.152) and (6.153) into Eq. (6.151), we have the minimum noise figure

$$F_{min} = 1 + \left( \frac{1}{\beta_0} + \frac{2}{9} \omega^2 \tau_B^2 \right)^{1/2} , \quad (6.154)$$

where  $G_{EO} \simeq qI_C/k_B\theta$  is used and  $1/\beta_{00} \ll 1$  is neglected. At low frequencies,  $F_{min}$  reduces to  $1 + \beta_0^{-1/2}$ , which results in  $F=0.4$  dB for  $\beta = 100$ . At high frequencies,  $F_{min}$  increases with increasing frequency. In particular,  $F_{min}$  is proportional to  $\omega^2$  at medium frequencies where  $\omega \leq 9/(2\beta_0\tau_B^2)$ .

The above analysis does not include the finite base resistance and the excess noise caused by the generation-recombination process in the two depletion layers, but the noise analysis presented in this section is in good agreement with the observed noise behavior of the bipolar transistor. This means that a modern bipolar transistor comes already close to the ideal limit[4].

## 6.4 *pn* Junction Diodes Under Constant Current Operation

### 6.4.1 Effect of Finite Source Resistance

The origin of current noise in a constant-voltage-driven *pn* junction diode and bipolar transistor is the thermal diffusive transit between collisions with the lattice and the generation-recombination of a minority carrier (an electron in the *p*-layer or a hole in the *n*-layer). These events introduce the relaxation current in order to restore the steady-state distribution of minority carriers, which causes the departure of the minority carrier density at

the depletion layer edge. For instance, the temporal decrease in  $n_p$  in the  $p^+$ -layer in a  $p^+$ - $N$  junction results in excess forward thermionic emission from the  $N$ -layer to the  $p^+$ -layer, as compared to backward thermionic emission from the  $p^+$ -layer to the  $N$ -layer. This excess forward emission leads to the reduction of the electron density  $n_N$  at the other depletion layer edge in the  $N$ -layer. This departure of the electron density  $n_N$  from the steady-state value is eliminated immediately by a majority-carrier flow in the  $N$ -layer and subsequently in the external circuit. On the other hand, the temporal increase in  $n_p$  results in excess backward thermionic emission from the  $p^+$ -layer to the  $N$ -layer, which induces the increased electron density  $n_N$  and, thus, an opposite-polarity, external-circuit current flows.

When the voltage source has an infinitesimally small source resistance, the above relaxation process is completed with a negligible delay time. A system does not memorize a previous event of thermal diffusive transit or generation and recombination of a minority carrier. Therefore, each event occurs statistically independently and this independence is the physical origin for the full-shot noise of a  $pn$  junction diode under constant voltage operation, as shown in Fig. 6.15(a).

However, if the source resistance  $R_s$  is not negligibly small, the modulation in the density  $n_N$ , induced by excess forward or backward thermionic emission of an electron, cannot be instantaneously eliminated by an external circuit current. The junction voltage is now allowed to fluctuate by the thermal diffusive transit and generation-recombination events. If the recombination events for electrons in the  $p^+$ -layer exceed the average value, the junction voltage decreases due to excess forward thermionic emission of electrons. While this junction-voltage decrease is not eliminated by the external circuit relaxation current, the forward thermionic emission rate temporarily decreases and results in the lower recombination events of electrons in the  $p^+$ -layer. This sequence works as a self-feedback stabilization mechanism for regulating the recombination process in the  $p^+$ -layer. At the same time, the external circuit current is smoothed due to overlapping pulses with a long-relaxation time constant  $CR_s$ , as shown in Fig. 6.15(b).

A noise equivalent circuit of such a  $pn$  junction is already shown in Fig. 6.1, where  $C_{dep}$  is the depletion layer capacitance,  $C_{dif}$  is the diffusion capacitance,  $R_d$  is the differential resistance,  $i$  is the current noise source associated with  $R_d$ ,  $R_s$  is the source resistance, and  $i_s$  is the current noise source associated with  $R_s$ . The Kirchhoff circuit equation for this noise equivalent circuit is:

$$\frac{d}{dt}v_n = -\frac{v_n}{CR_s} + i_s - \frac{v_n}{CR_d} + i \quad , \quad (6.155)$$

where  $v_n$  is the junction voltage-fluctuation and  $C = C_{dep} + C_{dif}$  is the total junction capacitance. The first term on the right-hand-side of Eq. (6.155) is the relaxation (dissipation) rate of  $v_n$  due to an external circuit relaxation current and the second term is the Johnson-Nyquist thermal noise associated with  $R_s$  and its spectral density is  $S_{i_s}(\omega) = 4k_B\theta/R_s$ . The third term on the right-hand-side of Eq. (6.155) is the relaxation (dissipation) rate of  $v_n$  due to thermionic emission of electrons across the depletion layer and/or recombination of electrons and the fourth term is the noise current associated with thermionic emission and/or recombination.

There are two operational modes of  $pn$  junction diodes, as illustrated in Fig. 6.15.

(1)  $R_s \ll R$  (Constant Voltage Operation)

The junction voltage fluctuation induced by forward/backward thermionic emission and generation-recombination of electrons is instantaneously eliminated by the external circuit relaxation current pulse; thus  $v_n \rightarrow 0$ . The system does not have a memory effect for thermal diffusion and generation-recombination events of minority carriers, so the noise current associated with these events features full-shot noise,  $\overline{S_i(\omega)} = 2qI$ , as demonstrated in the previous section.

(2)  $R_s \gg R$  (Constant Current Operation)

The external circuit current fluctuation is smoothed by a slow relaxation current pulse due to a large source resistance  $R_s$ . The thermionic emission process becomes regulated by the self-feedback mechanism mentioned above. Therefore,  $S_i(\omega)$  is expected to feature a sub-shot-noise character, but the junction voltage fluctuation  $v_n$  is not suppressed.

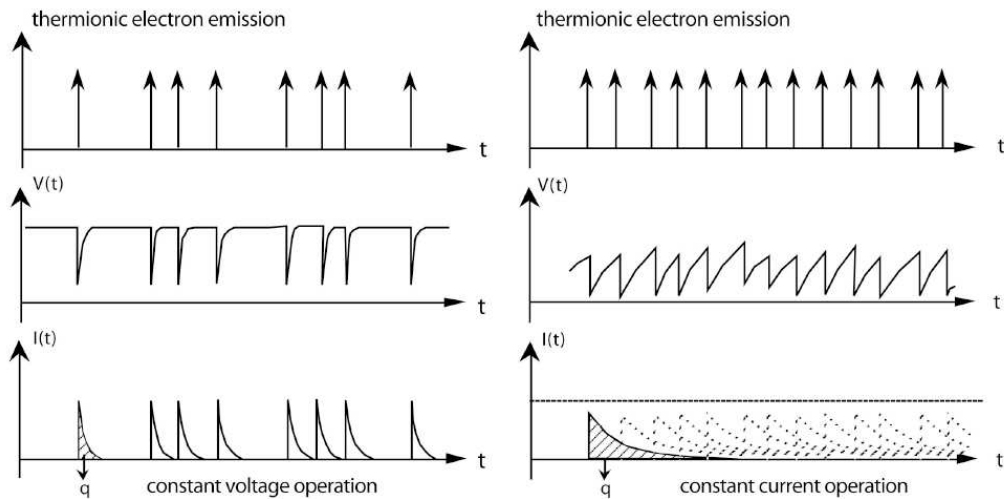


Figure 6.15: Constant voltage operation (a) and constant current operation (b) of a  $pn$  junction diode.

A  $pn$  junction diode under a strong forward bias condition often has a negligible differential resistance,  $R_d = \frac{V_T}{I}$ , compared to the source resistance  $R_s$ . A semiconductor light emitting diode and laser are such examples. In such devices, the junction current noise is lower than the standard full shot noise and the emitted photon flux also features a sub-shot noise behaviour[6].

## 6.4.2 Current Noise Spectral Density

Let us consider the situation where a  $pn$  junction is driven by a voltage source with a series resistance  $R_s$ . A noise equivalent circuit is shown in Fig. 6.1, as already mentioned.

Taking the Fourier transform of Eq. (6.155), we obtain

$$\left(i\omega C + \frac{1}{R_s} + \frac{1}{R_d}\right) V_n(\omega) = I(\omega) - I_s(\omega) \quad , \quad (6.156)$$

where  $V_n(\omega)$ ,  $I_s(\omega)$  and  $I(\omega)$  are now in their Fourier representations. The external circuit current noise  $I_n$  is obtained from the Kirchhoff's law:

$$I_n = -I_s - \frac{V_n}{R_s} \quad . \quad (6.157)$$

From Eqs. (6.156) and (6.157), we have

$$I_n(\omega) = \frac{-I(\omega) + \left(i\omega R_s C + \frac{R_s}{R_d}\right) I_s(\omega)}{i\omega R_s C + \frac{R_s}{R_d} + 1} \quad . \quad (6.158)$$

An external circuit current noise power spectral density is proportional to  $|I_n(\omega)|^2$ . Since the two noise sources  $i_s$  and  $i$  are independent and their respective power spectral densities are given by  $S_i(\omega) = 2qI$  and  $S_{i_s}(\omega) = 4k_B\Theta/R_s$ , we have

$$S_{in}(\omega) = \frac{2qI + \left[\left(\frac{R_s}{R_d}\right)^2 + (\omega R_s C)^2\right] 4k_B\Theta/R_s}{\left(1 + \frac{R_s}{R_d}\right)^2 + (\omega R_s C)^2} \quad . \quad (6.159)$$

Here, we assume strong forward bias, so  $I \sim I_s e^{qV/k_B\Theta}$ . The diode resistance is then well approximated by  $R_d = I/V_T$ , and consequently,  $2qI = \frac{2k_B\Theta}{R_d}$ . We now look at two limits.

- i) Constant voltage source:  $R_s \ll R_d$ ,  $2qI = 2k_B\Theta/R_d \ll 4k_B\Theta/R_s$   
Under this condition, the noise spectral density is reduced to

$$S_{in}(\omega) = \frac{2qI + (\omega C R_s)^2 \frac{4k_B\Theta}{R_s}}{1 + (\omega C R_s)^2} \quad . \quad (6.160)$$

In a low frequency limit ( $\omega C R_s \ll 1$ ), we recover the full shot noise  $S_{in}(\omega) = 2qI$ . However, in an opposite limit ( $\omega C R_s \gg 1$ ), we have the thermal noise current  $S_{in}(\omega) = 4k_B\Theta/R_s$ . This is because at high frequencies, the  $pn$  junction is shorted by the junction capacitance  $C$  and the internal current noise  $i$  cannot be extracted to the external circuit.

- ii) Constant current source:  $R_s \gg R_d$ ,  $2qI = 2k_B\Theta/R_d \gg 4k_B\Theta/R_s$   
Under this condition, the noise spectral density is always the thermal noise limit:

$$S_{in}(\omega) = \frac{4k_B\Theta}{R_s} \quad . \quad (6.161)$$

### 6.4.3 Voltage Noise Spectral Density

The Fourier transformed terminal voltage  $V_n(\omega)$  of a  $pn$  junction is obtained from Eqs. (6.156) and (6.157):

$$V_n(\omega) = \frac{I(\omega) - I_s(\omega)}{\left(\frac{1}{R_s} + \frac{1}{R_d} + i\omega C\right)} \quad . \quad (6.162)$$

The power spectral density for the junction voltage noise is given by

$$S_{\text{vn}}(\omega) = \frac{2qIR_{\text{d}}^2 + 4k_{\text{B}}\Theta R_{\text{d}}^2/R_{\text{s}}}{\left(1 + \frac{R_{\text{d}}}{R_{\text{s}}}\right)^2 + (\omega R_{\text{d}}C)^2} . \quad (6.163)$$

We now look at two limits:

i) Constant voltage source:

Under this condition, we have

$$S_{\text{vn}}(\omega) = \frac{2qIR_{\text{s}}^2 + 4k_{\text{B}}\Theta R_{\text{s}}}{1 + (\omega R_{\text{s}}C)^2} , \quad (6.164)$$

and since  $2qIR_{\text{s}}^2 \ll 4k_{\text{B}}\Theta R_{\text{s}}$ ,

$$S_{\text{vn}}(\omega) = \frac{4k_{\text{B}}\Theta R_{\text{s}}}{1 + (\omega R_{\text{s}}C)^2} . \quad (6.165)$$

This is just the thermal noise associated with the source resistance and, as  $R_{\text{s}} \rightarrow 0$ , the junction voltage noise is suppressed.

ii) Constant current source:

Under this condition, we obtain

$$S_{\text{vn}}(\omega) = \frac{2qIR_{\text{s}}^2}{1 + (\omega R_{\text{d}}C)^2} . \quad (6.166)$$

If we normalize  $S_{\text{vn}}(\omega)$  by  $R_{\text{d}}^2$ , we have the full shot noise spectral density. However, this does not mean the junction current (or electron thermionic emission event) fluctuates according to the Poisson-point-process. Both electron emission and external current are regulated as shown in Fig. 6.15.

# Bibliography

- [1] W. Shockely, *Bell Syst. Tech. J.* **28**, 435 (1949).
- [2] R. M. Ryder and R. J. Kircher, *Bell Syst. Tech. J.* **28**, 367 (1949).
- [3] M. J. Buckingham, *Noise in Electronic Devices and Systems*, (Wiley, New York, 1983) Ch. 4.
- [4] S. M. Sze, *Physics of Semiconductor Devices*, (Wiley, New York, 1981) Ch. 3.
- [5] A. van der Ziel, *Noise in Solid State Devices and Circuits*, (Wiley, New York, 1986) Ch. 9.
- [6] Y. Yamamoto, *Coherence, Amplification and Quantum Effects in Semiconductor Lasers*, (Wiley, New York, 1991) Ch. 11.